JVI Journals.ASM.org

A Single-Amino-Acid Polymorphism in Chikungunya Virus E2 Glycoprotein Influences Glycosaminoglycan Utilization

Laurie A. Silva,[a,b] Solomiia Khomandiak,[a,b] Alison W. Ashbrook,[b,c] Romy Weller,[a,b]* Mark T. Heise,[d] Thomas E. Morrison,[e] Terence S. Dermody[a,b,c]

Departments of Pediatrics[a] and Pathology, Microbiology, and Immunology[c] and Elizabeth B. Lamb Center for Pediatric Research,[b] Vanderbilt University School of Medicine, Nashville, Tennessee, USA; Departments of Genetics and Microbiology and Immunology and Carolina Vaccine Institute, University of North Carolina—Chapel Hill, Chapel Hill, North Carolina, USA[d]; Departments of Microbiology and Immunology, University of Colorado School of Medicine, Aurora, Colorado, USA[e]

ABSTRACT

Chikungunya virus (CHIKV) is a reemerging arbovirus responsible for outbreaks of infection throughout Asia and Africa, causing an acute illness characterized by fever, rash, and polyarthralgia. Although CHIKV infects a broad range of host cells, little is known about how CHIKV binds and gains access to the target cell interior. In this study, we tested whether glycosaminoglycan (GAG) binding is required for efficient CHIKV replication using CHIKV vaccine strain 181/25 and clinical isolate SL15649. Preincubation of strain 181/25, but not SL15649, with soluble GAGs resulted in dose-dependent inhibition of infection. While parental Chinese hamster ovary (CHO) cells are permissive for both strains, neither strain efficiently bound to or infected mutant CHO cells devoid of GAG expression. Although GAGs appear to be required for efficient binding of both strains, they exhibit differential requirements for GAGs, as SL15649 readily infected cells that express excess chondroitin sulfate but that are devoid of heparan sulfate, whereas 181/25 did not. We generated a panel of 181/25 and SL15649 variants containing reciprocal amino acid substitutions at positions 82 and 318 in the E2 glycoprotein. Reciprocal exchange at residue 82 resulted in a phenotype switch; Gly^{82} results in efficient infection of mutant CHO cells but a decrease in heparin binding, whereas Arg^{82} results in reduced infectivity of mutant cells and an increase in heparin binding. These results suggest that E2 residue 82 is a primary determinant of GAG utilization, which likely mediates attenuation of vaccine strain 181/25.

IMPORTANCE

Chikungunya virus (CHIKV) infection causes a debilitating rheumatic disease that can persist for months to years, and yet there are no licensed vaccines or antiviral therapies. Like other alphaviruses, CHIKV displays broad tissue tropism, which is thought to be influenced by virus-receptor interactions. In this study, we determined that cell-surface glycosaminoglycans are utilized by both a vaccine strain and a clinical isolate of CHIKV to mediate virus binding. We also identified an amino acid polymorphism in the viral E2 attachment protein that influences utilization of glycosaminoglycans. These data enhance an understanding of the viral and host determinants of CHIKV cell entry, which may foster development of new antivirals that act by blocking this key step in viral infection.

Chikungunya virus (CHIKV) is a reemerging arbovirus indigenous to Africa and Asia that causes Chikungunya fever in humans (1, 2). This illness is most often characterized by rapid onset of fever, incapacitating polyarthralgia, rash, myalgia, and headache (1–3). Although viremia is usually cleared 5 to 7 days after infection, a characteristic feature of CHIKV disease is recurring polyarthritis that can persist for months or years (4–8). Several *Aedes* species of mosquitoes serve as vectors of CHIKV, including *A. aegypti* and *A. albopictus* (9–12). CHIKV caused an explosive outbreak of disease beginning in 2004 that expanded to areas beyond the historical range of the virus, including Europe and many islands in the Indian Ocean (1, 2, 13), and produced more-severe illness than previously observed (14–17). CHIKV continues to spread to new regions (18–22), and currently there are no available vaccines or treatments for this disease (23).

CHIKV is a member of the *Togaviridae* and belongs to the Old World Semliki Forest virus (SFV) group of arthritogenic alphaviruses (reviewed in reference 24). The CHIKV genome is ~11.8 kb comprising a single-stranded, message-sense RNA molecule that is capped and polyadenylated (25). Viral proteins are synthesized as two independent polyprotein precursors that undergo proteolytic cleavage by viral and cellular proteases. The virion is a 70-nm-diameter, icosahedral, enveloped particle that contains three structural proteins, a capsid protein and two glycoproteins, E1 and E2 (26–29). E1 and E2 form heterodimers that associate in trimers, which constitute spikes on the viral envelope (28, 30). E1 is a class II viral fusion protein, while E2 mediates attachment of the virus to cells and is the most likely candidate for engagement of cell-surface receptors (29). After attachment and internalization, CHIKV is thought to enter the endocytic pathway, where E1 mediates fusion of the viral and endosomal membranes (31). This process is dependent on acidification of endosomal vesicles and most likely occurs in early endosomes in both mammalian and mosquito cells (13, 31–34).

Attachment to the host cell surface is the initial step in viral

Received 25 October 2013 **Accepted** 19 December 2013
Published ahead of print 26 December 2013
Editor: D. S. Lyles
Address correspondence to Terence S. Dermody, terry.dermody@vanderbilt.edu.
* Present address: Romy Weller, Institute of Virology and Cell Biology, University of Lübeck, Lübeck, Germany.

doi:10.1128/JVI.03116-13

infection and a critical determinant of tissue tropism. Many viruses use adhesion strengthening to engage cells via low-affinity tethering to common cell-surface molecules such as carbohydrates followed by binding to less-abundant, usually proteinaceous molecules with higher affinity (35, 36). A diverse array of viral pathogens, including adenovirus (37), coxsackievirus B3 variant PD (38), dengue virus (39), enterovirus 71 (40), herpes simplex virus (41), HIV-1 (42), human papillomavirus (43), and respiratory syncytial virus (44), use glycosaminoglycans (GAGs) as attachment factors. GAGs are negatively charged, unbranched linear carbohydrate polymers consisting of repeating disaccharide units made of glucuronic acid or iduronic acid, linked to an amino sugar, glucosamine or galactosamine. Types of GAGs include heparan sulfate, keratan sulfate, chondroitin sulfate, and dermatan sulfate. GAGs are found on the surface of most mammalian cell types and in the extracellular matrix. These molecules are involved in a number of biological functions, including embryonic development, cell adhesion, proliferation, migration, wound healing, and extracellular matrix assembly, among many others (reviewed in references 45 and 46). Most GAG-protein interactions are mediated between the negatively charged polysaccharide chain or sulfate groups of the GAG and clusters of basic amino acids, which may form a conformation-specific binding site, in the protein ligand (46–49).

Certain strains of several alphaviruses, including eastern equine encephalitis virus (EEEV) (50), Ross River virus (RRV) (51), Sindbis virus (SINV) (52, 53), SFV (54), and Venezuelan equine encephalitis virus (VEEV) (55), use glycosaminoglycans as attachment receptors. During cell culture adaptation of many alphaviruses, basic amino acids in E2 glycoproteins are rapidly selected (51–53, 55, 56). Concordantly, positively charged amino acid substitutions in E2 are implicated in mediating interactions with GAGs and in most cases with heparan sulfate (50–55, 57–62). Heparan sulfate binding by alphaviruses and other viruses often correlates with attenuation of disease in animal models (50, 55–59, 63), likely due to rapid clearance of the virus from the circulation of the infected animal (55, 58). However, natural isolates of EEEV display dependence on GAGs for infection of cells in culture, which correlates with increased neurovirulence (50). In addition, several low-passage-number strains of VEEV also exhibit different degrees of GAG dependence (62). Thus, GAG binding might confer some replicative advantage during infection with EEEV or VEEV and perhaps other alphaviruses as well. The role of GAGs in replication of CHIKV clinical isolates is not clear.

In this study, we examined whether a clinical isolate (SL15649) (64) or an attenuated, vaccine strain (181/25) (65) requires cell-surface GAGs for efficient attachment to target cells and subsequent infection. Strain SL15649 was isolated from a CHIKV-infected patient in Sri Lanka in 2006, has been minimally passaged in cell culture, and is pathogenic in a mouse model of CHIKV disease (64). Strain 181/25 was derived from strain AF15661, which was isolated from a patient in Thailand in 1962. Strain 181/25 was developed as a vaccine candidate for CHIKV by adapting AF15561 to cell culture by 18 plaque-to-plaque passages in a human lung fibroblast cell line (MRC-5) (65). In both mouse (76, 80) and nonhuman primate models, 181/25 is attenuated but immunogenic (65). In addition, administration of 181/25 protects against CHIKV challenge in nonhuman primates (65). Although 181/25 (called TSI-GSD-218) was highly immunogenic in phase II clinical trials, ~8% of vaccinees developed mild, transient arthralgia, suggesting partial or unstable attenuation (66, 67). Gardner et al. previously demonstrated that 181/25 infectivity was decreased in GAG-deficient Chinese hamster ovary (CHO) cells, suggesting that this laboratory-adapted strain is dependent on GAGs for infectivity (76). Here, we expanded upon previous studies and found that several GAGs competitively inhibit infectivity of BHK-21 cells by 181/25 but not SL16549. In contrast, both 181/25 and SL15649 depend on cell-surface GAGs for binding and infection of CHO cells. Furthermore, we identified residue 82 in the E2 glycoprotein as a key determinant of GAG utilization and binding to heparin by CHIKV. Collectively, these findings indicate that vaccine strain 181/25 is more dependent on GAGs than SL15649 for infectivity and suggest a mechanism of attenuation for 181/25.

MATERIALS AND METHODS

Cells and reagents. BHK-21 cells (ATCC CCL-10) were maintained in alpha minimal essential medium (αMEM; Gibco) supplemented to contain 10% fetal bovine serum (FBS) and 10% tryptose phosphate. Vero 81 cells (ATCC CCL-81) were maintained in αMEM supplemented to contain 5% FBS. Parental CHO-K1 and mutant CHO-pgsA745, CHO-pgsB761, and CHO-pgsD677 cell lines were maintained in Ham's F-12 nutrient mixture (Gibco) supplemented to contain 10% FBS. Media for all cells were supplemented with 0.29 mg/ml L-glutamine (Gibco), 100 U/ml penicillin (Gibco), 100 μg/ml streptomycin (Gibco), and 25 ng/ml amphotericin B. Cells were maintained at 37°C in an atmosphere of 5% CO_2. Parental CHO-K1 and CHO-pgsA745 cell lines were provided by Benhur Lee (University of California, Los Angeles). CHO-pgsB761 and CHO-pgsD677 cell lines were provided by Mark Peeples (The Research Institute at Nationwide Children's Hospital) with permission from Jeffrey Esko (University of California, San Diego). All chemicals were purchased from Sigma unless otherwise noted.

Biosafety. All studies using viable SL15649 and any mutant virus were conducted in a certified biological safety level 3 facility in biological safety cabinets with protocols approved by Vanderbilt University Department of Environment, Health, and Safety and the Vanderbilt Institutional Biosafety Committee.

Viruses. Virus stocks were generated from full-length wild-type (WT) and mutant virus infectious cDNA clones as described in references 64 and 68. Plasmids containing virus cDNAs were linearized by digestion with NotI-HF (NEB). Capped, full-length RNA transcripts were generated *in vitro* using mMessage mMachine SP6 transcription kits (Ambion) and introduced into BHK-21 cells by electroporation using a Gene Pulser electroporator (Bio-Rad). Culture supernatants were harvested 24 to 48 h after electroporation and clarified by centrifugation at 855 × *g* for 20 min. Virus stocks were purified by ultracentrifugation of clarified supernatants through a 20% sucrose cushion in TNE buffer (50 mM Tris-HCl [pH 7.2], 0.1 M NaCl, and 1 mM EDTA) at ~115,000 × *g* in a Beckman 32Ti rotor. Virus pellets were resuspended in virus dilution buffer (VDB; RPMI medium containing 20 mM HEPES [Gibco] supplemented to contain 1% FBS), aliquoted, and stored at −70°C. Virus titers were determined by plaque assay using Vero cells.

Assessment of CHIKV infectivity. BHK-21 cells (~4×10^3 cells/well) or CHO cells (~8×10^3 cells/well) were seeded into wells of 48-well plates (Costar) and incubated at 37°C for 24 h. Triplicate wells were inoculated with various virus strains at a multiplicity of infection (MOI) of 2.5 (BHK-21) or 10 (CHO) PFU/cell in VDB. Following adsorption at 37°C for 2 h, the inoculum was removed, and cells were incubated at 37°C for 18 h in complete medium containing 20 mM NH_4Cl (to block subsequent rounds of viral replication). Cells were washed twice with PBS, fixed in 100% ice-cold methanol, and incubated at −20°C for at least 20 min. Infected cells were visualized using indirect immunofluorescence. Cells were incubated in blocking buffer (phosphate-buffered saline [PBS; Gibco] containing 5% FBS and 0.1% Triton X-100) at room temperature for 1 h and stained with precleared anti-CHIKV immune ascetic fluid

(ATCC VR-1241AF) diluted 1:1,500 and secondary Alexa 488 goat anti-mouse antibody diluted 1:1,000 (Invitrogen), followed by addition of DAPI (4′,6-diamidino-2-phenylindole) to visualize cell nuclei. All antibodies were diluted in blocking buffer. For some experiments, cells were visualized using an Axiovert 200 fluorescence microscope (Zeiss). Total and CHIKV-infected cells were quantified using ImageJ software (69) in two fields of view per well. For other experiments, cells were visualized using an ImageExpress Micro XL imaging system (Molecular Devices) at the Vanderbilt High-Throughput Screening Facility. Total and CHIKV-infected cells were quantified using MetaExpress software (Molecular Devices) in two fields of view per well. No background stain was noted on uninfected control monolayers.

Infectivity inhibition assays. Purified CHIKV virions were pretreated with a range of dilutions of heparin, heparan sulfate, chondroitin sulfate A, chondroitin sulfate A/C/E from shark, dermatan sulfate, or hyaluronic acid at 4°C for 30 min before inoculation of BHK-21 monolayers with virus-GAG mixtures. For some experiments, bovine serum albumin (BSA) was included as a negative control. Following incubation at 37°C for 2 h, the inoculum was removed, and cells were incubated at 37°C for 18 h in complete medium with 20 mM NH_4Cl. Infectivity was quantified using indirect immunofluorescence.

Flow cytometric analysis of virus binding to cells. The effect of soluble GAGs on CHIKV binding to BHK-21 cells was determined by preincubating virus with GAGs in VDB at various concentrations at 4°C for 30 min. BHK-21 monolayers were washed and detached using Cellstripper (Cellgro), quenched with fluorescence-activated cell-sorting (FACS) buffer (PBS supplemented to contain 2% FBS), pelleted at 600 × *g*, washed once with PBS, and pelleted a second time at 600 × *g*. Cells (~1×10^5 to 3×10^5) were adsorbed with the virus-GAG mixtures at an MOI of 5 PFU/cell and incubated at 4°C for 30 min, washed twice in VDB, pelleted, and stained in VDB containing CHIKV-specific mouse monoclonal antibody CHK-187 (provided by Michael Diamond, Washington University). Cells were washed twice in VDB, pelleted, and stained in VDB containing Alexa Fluor 488-labeled goat anti-mouse IgG (Molecular Probes) at 4°C for 30 min. Cells were washed twice in VDB, pelleted, and fixed in FACS fix (PBS supplemented to contain 1% electron microscopy [EM]-grade paraformaldehyde [Electron Microscopy Sciences]). Cell-associated fluorescence was quantified using an LSRII flow cytometer (BD Biosciences, Vanderbilt University Flow Cytometry Shared Resource). The mean fluorescence intensity (MFI) of forward- and side-scatter gated populations was determined using FACSDiva software (BD Biosciences). Binding of pretreated virus to BHK-21 cells was normalized to binding of untreated virus controls and expressed as percent bound virus. Binding assays were performed using triplicate samples with at least 5×10^3 cells analyzed for each sample.

CHO cell monolayers were washed once with PBS and detached using Cellstripper (Cellgro) at 37°C, quenched with FACS buffer, pelleted at 600 × *g*, washed once with PBS, and pelleted a second time at 600 × *g*. Cells (~1×10^5 to 3×10^5) were adsorbed with virus at an MOI of 5 PFU/cell at 4°C for 1 h. Bound virus was quantified using flow cytometry. Binding of each virus to mutant CHO cells was normalized to virus bound to parental CHO-K1 cells and expressed as percent bound virus.

Kinetic heparan sulfate protection assay. Purified virions of strain 181/25 were adsorbed to monolayers of BHK-21 cells (~10^4) at an MOI of 2.5 PFU/cell. At 10 or 30 min prior to or 5, 10, 20, 30, or 45 min after adsorption, either heparan sulfate (250 μg/ml) or BSA (250 μg/ml) was added to the virus inoculum and rapidly mixed. Following incubation at 37°C for 2 h, the inoculum was removed, and cells were incubated at 37°C for 18 h in complete medium with 20 mM NH_4Cl. Infectivity was quantified using indirect immunofluorescence.

Kinetic ammonium chloride protection assay. Monolayers of BHK-21 cells (~10^4) seeded in 48-well plates were adsorbed with virus strains at an MOI of 2.5 PFU/cell and incubated at 37°C. At various times after adsorption, the inoculum was removed, and cells were incubated in complete medium containing 20 mM NH_4Cl at 37°C for 18 h. Infectivity was quantified using indirect immunofluorescence.

Generation of mutant viruses. Reciprocal single and double amino acid substitutions in the E2 glycoprotein were introduced into plasmids containing cDNAs of either strain 181/25 (p181/25 [68]) or SL15649 (pMH56.1 [64]) by PCR using mutagenic primers. Clones containing desired mutations were identified by DNA sequencing (GenHunter and Vanderbilt Sequencing Core) and digested with restriction endonucleases (SmaI and XhoI for p181/25 and SfiI and XhoI for pMH56.1). Mutagenized fragments were subcloned into unmodified versions of p181/25 or pMH56.1. Sequences of subcloned fragments of each mutant were determined to verify the fidelity of mutagenesis. Primer sequences for mutagenesis and sequencing are available from the corresponding author by request.

Genome-to-PFU ratios. The number of CHIKV genomes/ml for each purified virus stock was determined using reverse transcription-quantitative PCR (RT-qPCR). Viral RNA was extracted from 10 μl of purified virus stocks using TRIzol reagent (Life Technologies), purified using a PureLink RNA Minikit (Life Technologies), and eluted into a final volume of 100 μl. Quantification of the number of genomes in each virus stock was performed using a qScript XLT One-step RT-qPCR ToughMix kit (Quanta Biosciences) according to the manufacturer's instructions with minor modifications. Each 20-μl reaction mixture contained 5 μl viral RNA, 450 nM forward primer (SL15649for [874 5′-AAAGGGCAAACTC AGCTTCAC-3′] or 181-25for [5′-AAAGGGCAAGCTTAGCTTCAC-3′]), 900 nM reverse transcriptase and reverse primer (CHIKVrev [961 5′-GCCTGGGCTCATCGTTATTC-3′]), and 200 nM fluorogenic probe (CHIKVprobe [899 5′-6-carboxyfluorescein {dFAM}-CGCTGTGATAC AGTGGTTTCGTGTG-black hole quencher {BHQ}-3′]; Biosearch Technologies). Standard curves relating threshold cycle (C_T) values to copies of genomic RNA were generated from *in vitro*-transcribed genomic 181/25 or SL15649 RNA as described. Ten-fold dilutions of genomic RNA, from 10^{10} to 10^5 copies, were generated by calculating the number of genomes from *in vitro*-transcribed RNA by dividing the mass (measured by spectrometry [Nanodrop; Thermo Scientific]) by the genome molecular mass. RT-qPCR was performed using an Applied Biosystems 7500 Real-Time PCR system (Life Technologies, Foster City, CA) under the following cycling conditions: 50°C for 2 min, 95°C for 10 min, 40 cycles of 95°C for 15 s, and 60°C for 60 s, with data acquisition in the FAM channel during the 60°C step. The viral RNA concentration in each sample was determined by comparing C_T values of samples to the appropriate standard curve. Genome values per ml are expressed as the means of the results from two wells for three samples. Genome/PFU ratios are expressed as the mean number of genomes/ml divided by the mean number of PFU/ml for three RNA replicates using values from three plaque assay titrations.

Heparin-agarose-binding assay. Heparin-coated agarose beads or unconjugated beads were washed twice in PBS and twice in VDB. Washed beads (0.075 ml) were mixed with ~1×10^9 genomes of each virus in VDB and incubated with gentle agitation at 4°C for 30 min. Beads were washed three times in VDB and resuspended in 35 μl of 1× sample buffer (50 mM Tris-HCl [pH 6.8], 2% [wt/vol] sodium dodecyl sulfate [SDS], 1% β-mercaptoethanol, 6% [vol/vol] glycerol, 0.004% [wt/vol] bromophenol blue). Samples containing 12.5% of the input virus in 20 μl VDB were incubated with an equivalent volume of 2× sample buffer. All samples were boiled for 10 min, removed from the biosafety level 3 (BSL3) laboratory after disinfection, and stored at −70°C. Samples were resolved by SDS-polyacrylamide gel electrophoresis (PAGE) in 10% polyacrylamide gels (Bio-Rad) and transferred to an Immun-Blot polyvinylidene difluoride (PVDF) membrane (Bio-Rad). Membranes were incubated at room temperature for 1 h in blocking buffer (Tris-buffered saline [TBS] with 5% powdered milk), followed by incubation with mouse monoclonal antibody specific for CHIKV E2 (CHK 48-G8; provided by Michael Diamond, Washington University) diluted in TBS-T (TBS with 0.1% Tween 20) at 4°C overnight with gentle agitation. Membranes were washed with TBS-T three times for 5 min each time and incubated for 1 to 2 h with goat

anti-mouse secondary antibody conjugated to IRDye 800CW (Li-COR) dye diluted 1:2,000 in TBS-T at room temperature. Following three 5-min washes with TBS-T, membranes were rinsed twice with double-distilled water and scanned using an Odyssey imaging system (Li-COR).

Structural and sequence analysis. The crystallographic structure of the CHIKV E1/E2 trimer placed into the Sindbis virus cryo-EM map (Protein Data Base [PDB] accession no. 2XFB [30]) was used as a template to model the electrostatic surface potential of the E1/E2 trimers of SL15649 and 181/25. Coot (70) was used to alter 12 of the 16 amino acids within E2 that are located in the crystal structure from SL15649 to 181/25 residues using the lowest free-energy rotamers. Electrostatic surface potentials for 181/25 and SL15649 were generated with the Adaptive Poisson-Boltzmann Solver (APBS) (71) using the PyMOL plug-in as implemented in PyMOL under dielectric constants of 2.0 and 80.0 for protein and solvent regions, respectively, and contoured at levels of ± 2.5 kT.

Amino acid sequences of the E2 protein from 158 CHIKV strains were aligned using data obtained from the NIAID Virus Pathogen Database and Analysis Resource (ViPR) (72) online through the web site at http://www.viprbrc.org.

Statistical analysis. Statistical analysis was performed using GraphPad Prism (Graphpad). Soluble-GAG competition assays and time course assays were evaluated for statistically significant differences by one-way analysis of variance (ANOVA) followed by Dunnett's *post hoc* test. Calculation of 50% inhibitory concentration (IC_{50}) values with 95% confidence intervals was facilitated using GraphPad Prism. Binding and infectivity assays with CHO cells and infectivity assays with mutant viruses were evaluated for statistically significant differences by one-way ANOVA followed by Tukey's multiple-comparison test. *P* values of <0.05 were considered to be statistically significant. All differences not specifically indicated to be significant were not significant ($P > 0.05$). All experiments were performed in triplicate at least twice.

RESULTS

Inhibition of strain 181/25 infectivity by soluble GAGs. We hypothesized that CHIKV vaccine strain 181/25 might have become adapted to use GAGs as attachment receptors during passage in cell culture, as has been demonstrated for other alphaviruses (51–53, 55). We also thought it possible that a clinical isolate of CHIKV could use GAGs for infectivity, as has been noted for natural isolates of EEEV and VEEV (50, 62). To assess whether soluble GAGs act as competitive agonists and block infectivity of CHIKV strains 181/25 and SL15649, we performed competition assays using increasing concentrations of different GAGs. Purified 181/25 or SL16549 virions were preincubated with heparin, heparan sulfate, chondroitin sulfate A, dermatan sulfate, hyaluronic acid, shark cartilage chondroitin sulfate, or bovine serum albumin and adsorbed to BHK-21 cells. Cells were scored for infectivity in a single-round replication assay using indirect immunofluorescence. Preincubation of 181/25 with heparin, heparan sulfate, chondroitin sulfate A, or dermatan sulfate decreased infectivity of BHK-21 cells in a dose-dependent manner (Fig. 1A). Dermatan sulfate and heparan sulfate were the most potent inhibitors of 181/25 infectivity in this assay. Chondroitin sulfate A and heparin were also potent inhibitors of 181/25 infectivity. Hyaluronic acid and a mixture of chondroitin sulfate A/C/E from shark cartilage also inhibited 181/25 in a dose-dependent manner (Table 1 and data not shown). As a control, BSA did not significantly diminish infectivity at any dose tested (Fig. 1A). In addition, heparin inhibited 181/25 plaque formation in a dose-dependent manner using plaque-reduction assays (data not shown). We also tested whether heparin preincubation could inhibit 181/25 produced by C6/36 mosquito cells and found that mosquito-derived virus was inhibited by this soluble GAG in a dose-dependent manner and to an extent similar to that seen with mammalian-derived 181/25 (data not shown). Preincubation of 181/25 with soluble GAGs also inhibited infectivity of CHO-K1 cells (data not shown), indicating that the inhibitory effect of GAGs on 181/25 infectivity is not restricted to BHK-21 cells. Importantly, preincubation of cells with 500 μg/ml of heparin, heparan sulfate, chondroitin sulfate A, dermatan sulfate, and hyaluronic acid prior to viral infection did not inhibit infectivity of 181/25 (data not shown). These results indicate that the inhibitory effect of soluble GAGs is due to interactions with virus and not cells.

In contrast to the 181/25 results, the infectivity of strain SL15649 was not significantly altered in a dose-dependent manner by any of the soluble GAGs tested (Fig. 1B and data not shown). These data indicate that 181/25 and SL15649 differ in susceptibility to inhibition by soluble GAGs and suggest that these CHIKV strains exhibit differential interactions with GAGs, possibly in the affinity for GAGs or in the nature of GAG interactions.

Since the infectivity of strain 181/25 was efficiently inhibited by GAGs, we next tested whether incubation of virus with soluble GAGs blocks binding of 181/25 to BHK-21 cells. Purified 181/25 virions were incubated with soluble GAGs prior to adsorption to BHK-21 cells. Virus binding was assessed using flow cytometry (Fig. 1C). Higher concentrations of GAGs were used in this assay since greater numbers of virion particles are required to detect a fluorescence signal following binding. Similar to the infectivity results, virus binding to BHK-21 cells was effectively blocked by preincubation with each of the GAGs tested in a dose-dependent manner. In this assay, heparin was the most potent inhibitor of binding of 181/25 to BHK-21 cells. Dermatan sulfate and heparan sulfate also inhibited binding, as did chondroitin sulfate A, but at much higher concentrations (Table 1). Differences in the magnitude of inhibition by specific soluble GAGs in the infectivity and binding assays are likely due to differences in assay conditions, including cell number, virus concentration, temperature, and duration of adsorption. Collectively, these data indicate that soluble GAGs inhibit infectivity of strain 181/25, but not SL15649, on BHK-21 cells by blocking 181/25 from binding to the cell surface and suggest that 181/25 and GAGs directly interact.

Inhibition of 181/25 by soluble heparan sulfate occurs prior to endosomal escape. To determine whether inhibition of 181/25 infectivity by soluble GAGs occurs during an early step of the entry process prior to endosomal escape, we defined the temporal window at which heparan sulfate acts by adding the GAG to virus inocula at various times during the adsorption phase. Consistent with our previous observations (Fig. 1A), incubation of 181/25 with heparan sulfate prior to adsorption resulted in almost complete inhibition of 181/25 infectivity (Fig. 2A), whereas incubation with BSA had no effect (data not shown). Inhibition of 181/25 infectivity by heparan sulfate diminished as a function of time following viral adsorption. Notably, almost 50% of the inhibitory effect of heparan sulfate was lost when it was added 20 min post-adsorption (~56% infected cells; $P < 0.01$ compared with the BSA control). When added 45 min after adsorption, heparan sulfate lost almost all inhibitory effect (~88% infected cells; $P < 0.01$ compared with the BSA control). These data indicate that heparan sulfate inhibits 181/25 infectivity early in the infectious cycle.

Since attachment of CHIKV occurs prior to internalization of the virus into the endocytic pathway, we sought to determine the time required for 181/25 to escape the endosome and become resistant to a lysosomotropic agent. We assessed the capacity of

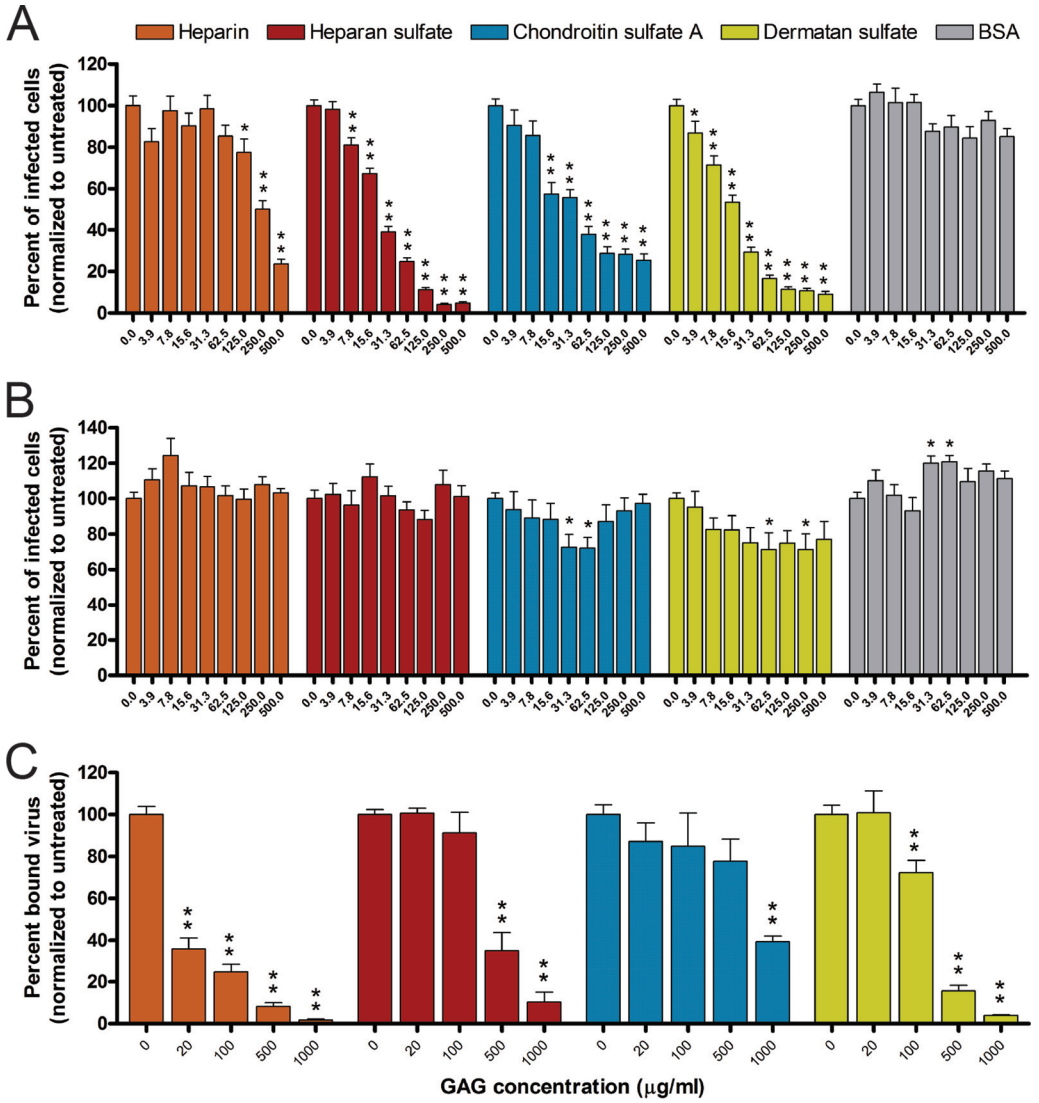

FIG 1 Soluble GAGs inhibit 181/25 infectivity and binding. (A and B) Purified virions of strain 181/25 (A) or SL15649 (B) (MOI of ~2.5 PFU/cell) were incubated with buffer alone or buffer containing heparin, heparan sulfate, chondroitin sulfate A, dermatan sulfate, or bovine serum albumin (BSA) at the concentrations shown at 4°C for 30 min prior to adsorption to BHK-21 cells. At 2 hpi, the inoculum was replaced with medium containing 20 mM NH_4Cl. At 18 hpi, infected cells were detected by indirect immunofluorescence. Results are expressed as the mean percentage of infected cells normalized to untreated controls for three (181/25) or two (SL15649) independent experiments performed in triplicate. Error bars indicate SEM. *, $P < 0.05$; **, $P < 0.01$ (in comparison to untreated controls as determined by one-way ANOVA followed by Dunnett's *post hoc* test). (C) Strain 181/25 (MOI of ~5 PFU/cell) was incubated with buffer alone or buffer containing heparin, heparan sulfate, chondroitin sulfate A, or dermatan sulfate at the concentrations shown at 4°C for 30 min. Virus-GAG mixtures were adsorbed to BHK-21 cells at 4°C for 30 min and stained with a CHIKV-specific antibody. The MFI of each sample was determined by flow cytometry. The data were normalized to the MFI of untreated virus controls for three independent experiments performed in triplicate. Error bars indicate SEM. *, $P < 0.01$ (in comparison to untreated controls as determined by one-way ANOVA followed by Dunnett's *post hoc* test).

NH_4Cl to inhibit 181/25 infectivity of BHK-21 cells when added at various times during the adsorption phase (Fig. 2B). NH_4Cl raises the pH of intracellular organelles within 1 min following addition to the medium (73), thereby allowing inhibition of low-pH-dependent endosomal escape by the virus at defined intervals postinfection. BHK-21 cells were adsorbed with 181/25 virions, and medium containing 20 mM NH_4Cl was added at various intervals after adsorption. The percent infected cells at 18 hours postinfection (hpi) was determined by indirect immunofluorescence and normalized to the infectivity of 181/25 when NH_4Cl was added at 120 min after infection. When NH_4Cl was added at 5 min postadsorption, only 4.5% of cells were infected by 181/25 ($P < 0.01$). Inhibition of 181/25 infectivity by NH_4Cl decreased gradually over time, with approximately half of the inhibitory effect lost by 45 min postadsorption ($P < 0.01$) and all the inhibitory effect lost by 100 min postadsorption ($P > 0.05$). These data confirm previous observations that endosomal acidification is essential for CHIKV infection of cells (13, 31–34) and suggest that inhibition of 181/25 infectivity by heparan sulfate occurs prior to inhibition by NH_4Cl.

CHIKV strains 181/25 and SL15649 require cell-surface GAGs for binding and infectivity. To examine whether GAGs are required for CHIKV infection, we tested 181/25 and SL15649 for the capacity to infect parental CHO-K1 cells and a panel of mutant

TABLE 1 Inhibition of 181/25 infectivity and binding by soluble GAGs

Inhibitor	Infectivity		Binding	
	Inhibition (%)[a]	IC_{50}, μg/ml (95% CI)[b]	Inhibition (%)[c]	IC_{50}, μg/ml (95% CI)[b]
Heparin	76.4 ± 9.8	248.5 (203.6–303.5)	98.3 ± 1.3	7.9 (3.542–17.74)
Heparan sulfate	95.1 ± 3.4	25.3 (23.3–27.5)	90.9 ± 11.4	357.7 (254.0–503.7)
Chondroitin sulfate A	74.6 ± 13.3	44.5 (34.4–57.5)	96.0 ± 0.6	179.1 (130.6–245.7)
Dermatan sulfate	90.9 ± 6.9	17.5 (15.21–19.35)	60.6 ± 6.5	>750[d]
Chondroitin sulfate A/C/E	78.2 ± 11.0	9.0 (6.469–12.52)	ND[e]	ND
Hyaluronic acid	86.7 ± 8.6	112.3 (97.9–128.8)	ND	ND

[a] Percent inhibition of infectivity compared with untreated controls (at a concentration of inhibitor of 500 μg/ml) ± standard error of the mean.
[b] Inhibitory concentration of each GAG that prevents 50% of infectivity (IC_{50}) relative to untreated controls with the 95% confidence interval (CI).
[c] Percent inhibition of binding compared with controls (at a concentration of inhibitor of 1,000 μg/ml) ± standard error of the mean.
[d] Could not be determined accurately due to partial dose response.
[e] ND, not determined.

CHO cells that display various defects in GAG biosynthesis (Fig. 3A). Parental CHO-K1 and mutant cell lines were adsorbed with either strain and scored for infectivity using conditions to allow a single infectious cycle. Cell line pgsA745, which is deficient in xylosyltransferase activity and thus lacks expression of all GAGs (74, 75), was highly resistant to infection by 181/25 (~0.5% infected cells; $P < 0.001$ compared with the CHO-K1 cells), confirming previous observations (76). These cells also were resistant to infection by SL15649 (~18% infected cells; $P < 0.001$ compared with the CHO-K1 cells). pgsA745 cells were less susceptible to strain 181/25 than to strain SL1649 ($P < 0.001$), suggesting that 181/25 is more dependent than SL15649 on GAGs for efficient infection. Cell line pgsB761, which is deficient in galactosyltransferase I and expresses only ~5% of the wild-type levels of heparan sulfate and chondroitin sulfate (75), was highly resistant to 181/25 infection (~7% infected cells; $P < 0.001$) but highly susceptible to SL15649 infection, with the infectivity level nearing that of parental CHO-K1 cells (~97% infected cells; $P > 0.05$). Similarly, cell line pgsD677, which is deficient in both N-acetylglucosaminyltransferase and glucuronosyltransferase activity and produces a 3-fold excess of chondroitin sulfate but no heparan sulfate (77), was highly resistant to 181/25 (~2% infected cells; $P < 0.001$) but susceptible to SL15649 (~70% infected cells; $P < 0.001$), albeit less susceptible than the pgsB761 cell line. These results suggest that both vaccine strain 181/25 and clinical isolate SL15649 depend on cell-surface GAGs for efficient infection but that the specific GAGs or structural specificities of the GAGs used by these viruses may differ.

To determine whether GAGs are required for attachment of 181/25 and SL15649 to CHO cells, we tested both viruses for the capacity to bind parental and mutant CHO cell lines. Cells were incubated with either virus strain and scored for binding using flow cytometry (Fig. 3B). Strain 181/25 did not efficiently bind to any of the mutant cell lines ($P < 0.001$ for pgsA745, pgsB761, and pgsD677 compared with CHO-K1). In contrast, SL15649 bound modestly to both pgsB761 and pgsD677 cells ($P < 0.001$ for both cell lines compared with CHO-K1) but less well to pgsA745 cells ($P < 0.001$ compared with CHO-K1). To confirm that CHO-K1 and mutant cell lines can support viral replication if entry steps are bypassed, we introduced *in vitro*-transcribed 181/25 RNA into both CHO-K1 and pgsA745 cells by electroporation and determined titers of progeny virus in cell supernatants 24 h later. We found that CHO-K1 and pgsA745 cells produce infectious virus to similar extents following viral RNA electroporation (data not

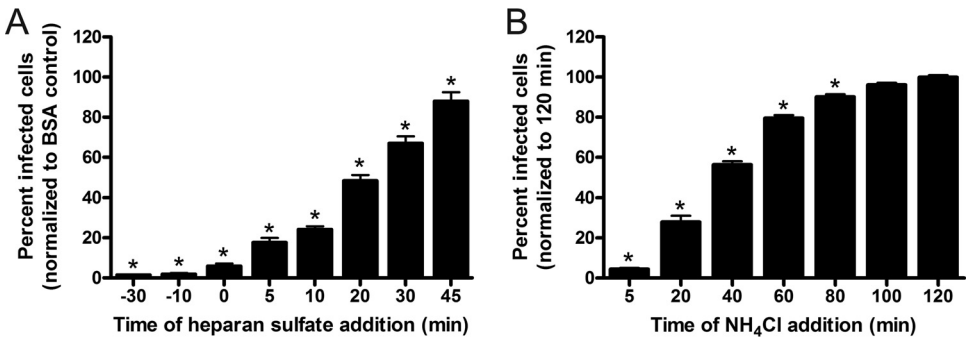

FIG 2 Kinetics of inhibition of 181/25 by heparan sulfate and ammonium chloride. (A) 181/25 virions (MOI of ~2.5 PFU/cell) were adsorbed to BHK-21 cells at 37°C. At the times shown prior to or during adsorption, heparan sulfate (250 μg/ml) was added to the virus inoculum. After 2 h adsorption, unbound virus was removed, and cells were incubated with medium containing 20 mM NH_4Cl. At 18 hpi, infected cells were detected by indirect immunofluorescence. Results are expressed as the mean percentage of infected cells normalized to BSA-treated controls from two independent experiments performed in triplicate. Error bars indicate SEM. *, $P < 0.01$ (in comparison to BSA-treated controls as determined by one-way ANOVA followed by Dunnett's *post hoc* test). (B) 181/25 virions (MOI of ~2.5 PFU/cell) were adsorbed to BHK-21 cells at 37°C. At the times shown following adsorption, the virus inoculum was removed, and cells were incubated with medium containing 20 mM NH_4Cl. At 18 hpi, infected cells were detected by indirect immunofluorescence using a CHIKV-specific polyclonal antibody. Results are expressed as the mean percentage of infected cells normalized to the percentage of infected cells when NH_4Cl was added at 120 min from three independent experiments performed in triplicate. Error bars indicate SEM. *, $P < 0.01$ (in comparison to untreated controls as determined by one-way ANOVA followed by Dunnett's *post hoc* test).

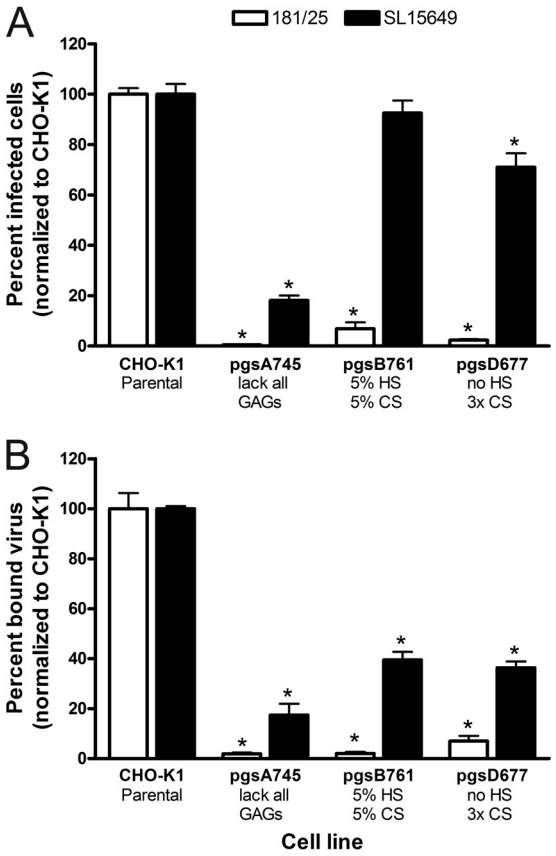

FIG 3 CHIKV 181/25 and SL15649 infectivity of and binding to parental and mutant CHO cells. (A) Parental CHO-K1, pgsA745, pgsB761, and pgsD677 cells were adsorbed with an MOI of ~10 PFU/cell of either 181/25 or SL15649. At 2 hpi, the inocula were replaced with medium containing 20 mM NH_4Cl. At 18 hpi, infected cells were detected by indirect immunofluorescence. Results are expressed as the mean percentage of infected cells normalized to the percentage of infected parental CHO-K1 cells for three (181/25) or two (SL15649) independent experiments performed in triplicate. Error bars indicate SEM. *, $P < 0.001$ (in comparison to the infectivity of the appropriate parental virus in CHO-K1 cells as determined by one-way ANOVA followed by Tukey's multiple-comparison test). (B) Parental CHO-K1, pgsA745, pgsB761, and pgsD677 cells were adsorbed with an MOI of ~5 PFU/cell of either 181/25 or SL15649 at 4°C for 1 h and stained with a CHIKV-specific antibody. The mean fluorescence intensity (MFI) of each sample was determined by flow cytometry. The data were normalized to the MFI of virus bound to parental CHO-K1 cells for three (181/25) or two (SL15649) independent experiments performed in triplicate. Error bars indicate SEM. *, $P < 0.001$ (in comparison to the binding of the appropriate parental virus to CHO-K1 cells as determined by one-way ANOVA followed by Tukey's multiple-comparison test). GAG, glycosaminoglycan; HS, heparan sulfate; CS, chondroitin sulfate.

shown). Together, these data indicate that both vaccine strain 181/25 and clinical isolate SL15649 depend on cell-surface GAGs for infection, specifically at the stage of viral attachment.

E2 residue 82 influences dependence on cell-surface GAGs. Although both 181/25 and SL15649 depend to some extent on cell-surface GAGs for efficient binding and infectivity, these strains display differences in the requirement for GAG utilization and inhibition by soluble GAGs. To identify amino acids responsible for these differences, we compared E2 amino acid sequences of 181/25 and SL15649 and found 16 amino acid polymorphisms (Table 2). Interestingly, 181/25 E2 contains arginines at residues 82 and 318, whereas SL15649 E2 contains glycine and valine residues at these positions, respectively. We were particularly interested in residue 82 because the presence of an arginine at this position is partially responsible for attenuation of virulent strains in some mouse models of CHIKV infection (80). To determine whether differences in GAG utilization between 181/25 and SL15649 are due to polymorphisms at one or both of these positions, we generated isogenic variants in the SL15649 and 181/25 infectious clones containing reciprocal amino acid substitutions at residues 82 and 382 in single- and double-mutant constructs (Table 3). The rescued viruses were viable, producing cytopathic effect (CPE) in BHK-21 cells within 24 h of electroporation and replicating to titers of 10^7 to 10^9 PFU/ml of purified virus, which are comparable to those seen with the parental SL15649 and 181/25 viruses, respectively (Table 3). In these experiments, we observed a correlation between virus titers in Vero cells and the amino acid at position 82. 181/25-E2 R82G and -E2 R82G/R318V virus titers were approximately 6- to 8-fold lower than those of 181/25. Correspondingly, SL15649-E2 G82R and -E2 G82R/V318R virus titers were approximately 5- to 7-fold higher than titers of SL15649. Titers for the reciprocal E2 318 mutants were comparable to those of their parental counterparts. We also observed a small-plaque phenotype for SL15649-E2 G82R and -E2 G82R/V318R compared with SL15649 (data not shown). Of note,

TABLE 3 CHIKV parental and mutant viruses used in this study

Virus	No. of genomes/ml[a]	PFU/ml[b]	Genome/PFU ratio	Normalized ratio[c]
181/25				
WT	1.58×10^{11}	1.4×10^{9}	120	1.0
E2 R82G	7.88×10^{10}	2.2×10^{8}	360	3.2
E2 R318V	7.22×10^{10}	1.0×10^{9}	72	0.62
E2 R82G/R318V	8.83×10^{10}	1.8×10^{8}	500	4.4
SL15649				
WT	7.71×10^{10}	1.7×10^{7}	4400	1.0
E2 G82R	1.93×10^{10}	1.2×10^{8}	160	0.036
E2 V318R	1.51×10^{11}	3.0×10^{7}	5100	1.1
E2 G82R/V318R	2.91×10^{10}	8.3×10^{7}	350	0.079

[a] Genomes/ml data were determined by duplicate real-time quantitative PCRs from three replicate experiments.
[b] Titers were determined by plaque assay using Vero cells. The mean viral titers from three independent plaque assays of a single stock are shown.
[c] Each mutant genome/PFU value was normalized to the parental WT value. The ratio of the relative numbers of genomes to PFU of WT 181/25 to that of WT SL15649 was 0.027.

TABLE 2 Amino acid polymorphisms in the E2 glycoprotein sequences of viruses used in this study

Virus strain	E2 amino acid at position[a]: 2	12	82	118	149	157	164	194	205	255	312	317	318	375	377	384
SL15649	T	T	G	S	K	V	T	G	G	I	M	V	V	T	I	M
181/25	I	I	R	G	R	A	A	S	D	V	T	I	R	S	V	V

[a] Numbered from the N terminus of E2.

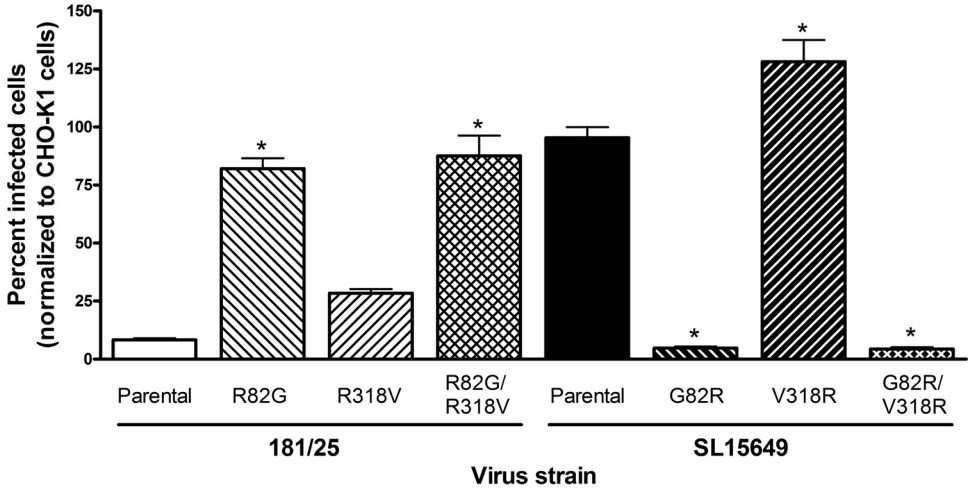

FIG 4 E2 residue 82 is a primary determinant of GAG utilization. Parental CHO-K1 and pgsB761 cells were adsorbed with an MOI of ~10 PFU/cell of each parental virus (181/25 or SL15649) or the E2 mutants shown. At 2 hpi, the inoculum was replaced with medium containing 20 mM NH_4Cl. At 18 hpi, infected cells were detected by indirect immunofluorescence. Results are expressed as the mean percentage of infected pgsB71 cells normalized to parental CHO-K1 cells for each virus for two independent experiments performed in triplicate. Error bars indicate SEM. *, $P < 0.001$ (in comparison to infectivity of the appropriate parental virus in CHO-K1 cells as determined by one-way ANOVA followed by Tukey's multiple-comparison test).

a small-plaque phenotype was originally used as a criterion for selecting clone 181/25 (65). However, plaques formed by 181/25-E2 R82G and -E2 R82G/R318V were not correspondingly larger than those formed by 181/25 (data not shown).

As an additional measure of viral fitness, we determined the genome/PFU ratio for each virus in infectivity assays using Vero cells. The parental strains 181/25 and SL15649 had genome/PFU ratios of 120 and 4,400, respectively (Table 3). E2 318 mutants had genome/PFU ratios similar to those of the parental strains. However, variants 181/25-E2 R82G and 181/25-E2 R82G/R318V had genome/PFU values that were 3.2- and 4.4-fold higher, respectively, than those of 181/25. Correspondingly, SL15469-E2 G82R and SL15649-E2 G82R/V318R had genome/PFU ratios that were 28- and 13-fold lower, respectively, than those of SL15649. Thus, an arginine at position 82 in E2 results in increased viral titers, a decreased genome/PFU ratio, and, in the SL15649 background, a reduction in plaque size, suggesting that a basic residue at position 82 in E2 enhances viral fitness in mammalian cell culture. A small-plaque phenotype (51, 58, 59, 65) and a higher level of infectivity in cell culture (53, 61) have been observed with other GAG-binding alphavirus strains.

To determine whether either of the basic amino acids at E2 82 and 318 affects GAG utilization, parental and mutant viruses were tested for infection of parental CHO-K1 and mutant pgsB761 cells, the cell line in which we observed the greatest difference in infectivity between the two parental strains (Fig. 3A). As before, SL15649 efficiently infected pgsB761 cells (~95% infected), whereas infection of these cells was greatly impaired for 181/25 (~8%) relative to infection of parental CHO-K1 cells ($P < 0.001$ for both viruses) (Fig. 4). Substitution of Arg^{82} with a glycine in 181/25 E2 (181/25-E2 R82G) allowed efficient infection of pgsB761 cells (~82% infected; $P < 0.001$ compared with 181/25), whereas substitution of Gly^{82} in SL15649 E2 with an arginine (SL15649-E2 G82R) resulted in substantially reduced infectivity of these cells (~5% infected; $P < 0.001$ compared with SL15649). Substitution of Arg^{318} in 181/25 E2 with valine (181/25-E2 R318V) or of Val^{318} in SL15649 E2 with arginine (SL15649-E2 V318R) resulted in increased infectivity of pgsB761 cells (~28% or ~128% infected, respectively). The SL15649-E2 G82R/V318R double mutant did not efficiently infect pgsB761 cells (~4% infected; $P < 0.001$ compared with SL15649), whereas the 181/25-E2 R82G/R318V double mutant did (88% infected; $P < 0.001$ compared with 181/25), suggesting that the sequence polymorphism at residue 82 predominates in conferring infectivity of pgsB761 cells. Therefore, an arginine at E2 residue 82 yields a higher degree of dependence on cell-surface GAGs for efficient infection.

E2 R82 mediates a direct interaction with GAGs. Since cell-surface GAGs are required for efficient binding and infectivity by 181/25 and SL15649, we next tested whether CHIKV virions and GAGs directly interact. Equivalent genome copies (5×10^7) of purified 181/25, 181/25-E2 R82G, SL15649, or SL15649-E2 G82R virions were incubated with agarose beads conjugated to heparin or with unconjugated beads as a negative control, and bound material from both heparin-agarose and unconjugated beads was resolved by SDS-PAGE and transferred to a PVDF membrane. Membranes were immunoblotted using an anti-E2 antibody to detect captured virus. We found that 181/25 was efficiently captured by heparin-agarose beads, whereas 181/25-E2 R82G was not (Fig. 5A). Correspondingly, we observed little capture of SL15649 by heparin beads, while SL15649-E2 G82R was more efficiently precipitated (Fig. 5A). We detected no virus capture by beads alone, suggesting that interactions between heparin and virions are specific (Fig. 5B). Densitometric analysis of three independent experiments indicates that ~38% and ~24% of 181/25 and SL15649-E2 G82R, respectively, were captured by heparin-agarose beads (Fig. 5C). In contrast, SL15649 and 181/25-E2 G82R displayed low levels (~5%) of binding to heparin (Fig. 5C). We conclude that CHIKV virions directly interact with heparin and that this interaction is greatly enhanced by the presence of a basic residue at position 82 in the E2 glycoprotein.

Structural and sequence analysis of CHIKV E2 82. Since interactions between GAGs and proteins often occur via electrostatic and hydrogen-bond interactions between anionic (carboxylate and sulfate) groups in GAGs and cationic amino acid side

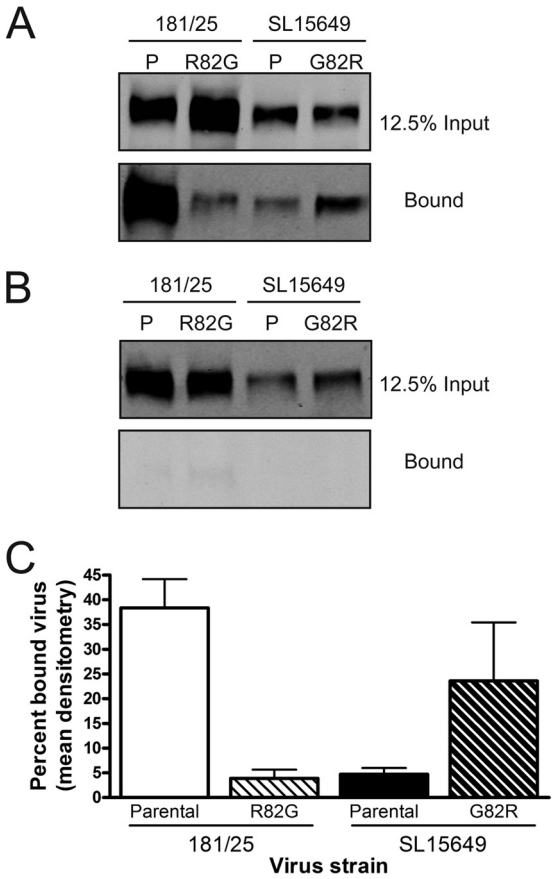

FIG 5 CHIKV E2 R82G mediates a direct interaction with heparin. Approximately 5×10^7 genome equivalents of purified 181/25, 181/25-E2 R82G, SL15649, and SL15649-E2 G82R virions were incubated with 75 μl of washed heparin-agarose beads (A) or unconjugated beads (B) at 4°C for 30 min. Beads were washed three times, and the bound material as well as 12.5% of the input virus was resolved by SDS-PAGE, transferred to a PVDF membrane, and immunoblotted for E2 as a marker for captured virus using a CHIKV-specific monoclonal antibody. The results of an experiment representative of three performed are shown. P, parental virus. (C) Densitometric analysis of virus bound to heparin-agarose beads. Data are expressed as the mean percent bound virus calculated from the densitometric analysis of captured virus divided by the estimated total input virus for three independent experiments. Error bars indicate SEM.

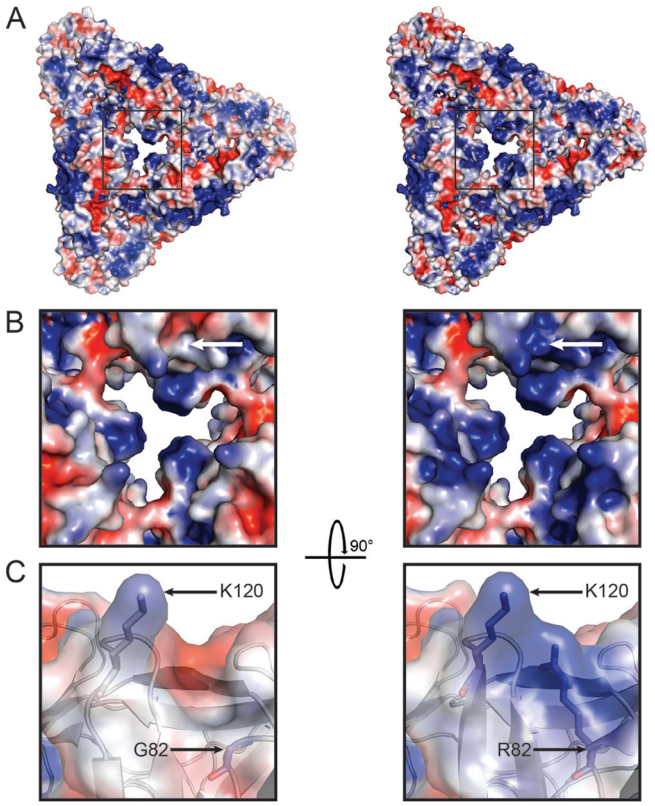

FIG 6 Electrostatic potentials of SL15649 and 181/25 E1/E2 trimers. (A) Top view of the electrostatic potential map displayed on the molecular surface of E1/E2 trimers of SL15649 (left panel) compared with a model of 181/25 (right panel) based on the crystal structure of CHIKV E1/E2 (PDB accession no. 2XFB). Positive potential is depicted in blue, and negative potential is depicted in red. (B) Enlarged view of the boxed areas from panel A highlighting the central cavity of the E1/E2 trimer. A white arrow indicates the position of Gly^{82} in SL15649 (left panel) or Arg^{82} in 181/25 (right panel) in one of the E2 monomers. (C) Enlarged view of the inner cavity rotated by 90° around the horizontal axis from the top view in panel B. A ribbon tracing of E2 is shown with a semitransparent view of the electrostatic surface and amino acids Gly^{82} (SL15649, left panel) or Arg^{82} (181/25, right panel) and Lys^{120} shown in stick representations.

chains, we sought to determine how substitution of Gly^{82} to Arg affects the local electrostatic environment surrounding this residue. Using the crystal structure of the CHIKV E1/E2 trimer (Protein Data Bank [PDB] accession code 2XFB [30]), we modeled the 181/25 E2 structure by substituting 12 residues of the 16 total polymorphisms displayed by the two strains (Table 2) located within the crystal structure, including G82R. The electrostatic charge distribution for each virus was calculated using the PyMol plug-in program APBS (71) and mapped onto a molecular surface representation of the E1/E2 trimer (Fig. 6). In the SL15649 model of the E1/E2 trimer (Fig. 6A and B, left panels), Gly^{82} is located in the "wings" insertion in the BC loop at the top of the immunoglobulin-like β-barrel fold that comprises domain A of E2, which has been implicated in mediating interactions with receptors (30). Gly^{82} is part of a cavity formed by domain A, which is centered on the 3-fold axis of the trimer spike. The three Gly^{82} residues are located at the inner apical surface of the cavity, facing toward the cavity center (Fig. 6A and B). Substitution of glycine with an arginine at residue 82 results in an expected increase in positive charge of the environment surrounding this residue (Fig. 6B). In addition, the additional density of the larger arginine side chain occupies a space adjacent to a conserved lysine at position 120, which is vacant in the SL16549 structure (Fig. 6C). Since residue 82 is part of the central cavity, it is possible that the increase in positive charge at this position in 181/25 results in formation of a GAG-binding pocket at the central cavity apex.

We surveyed the frequency of an arginine or glycine at E2 82 in historical and circulating CHIKV strains. Alignment of the 158 CHIKV E2 protein sequences available in the NIAID ViPR database (72) revealed that 157 of 158 (>99%) sequences contained a glycine at position 82 in E2. The only sequence in the database that contains an arginine at this residue is 181/25 (TSI-GSD-218 [65, 67]). CHIKV11, a strain isolated from an infected patient in Singapore in 2006, is the only other published CHIKV strain that has an arginine at position 82 in E2 (78). CHIKV11 was passaged in Vero cells and may have acquired an arginine at position 82 during cell-culture passage (78). This analysis reveals that a glycine at residue 82 in E2 is highly conserved.

DISCUSSION

The initial events in the replication cycle of CHIKV are not well defined. In this study, we found that CHIKV vaccine strain 181/25 requires cell-surface glycosaminoglycans for efficient attachment to and infection of cells in culture. In addition to pgsA745 cells, which are not susceptible to 181/25 infection (76), pgsB761 cells or pgsD677 cells are likewise not susceptible to 181/25 infection, suggesting that 181/25 is dependent on cell-surface heparan sulfate for efficient infection. We detected decreased cell binding by 181/25 both in the absence of cell-surface GAGs and in the presence of soluble GAGs. Moreover, we found that inhibition of 181/25 infectivity by soluble heparan sulfate occurs prior to endosomal escape. Collectively, these data suggest that 181/25 uses heparan sulfate proteoglycans as attachment receptors.

Our structural analysis suggests that Arg^{82} participates in a solvent-accessible GAG-binding pocket in the central cavity of the E1/E2 trimer of 181/25. Although the precise GAG-binding site cannot be determined without high-resolution structural studies of 181/25 with a soluble GAG, it is likely that a number of basic amino acids in E2 coordinate interactions with GAGs (46, 49, 79). We think it likely that Arg^{82} participates in a network of basic residues, possibly including Lys^{120}, which form a GAG-binding site in 181/25 E2 and enhances the affinity of the glycoprotein for GAGs. In support of this model, 181/25 bound heparin more efficiently than did SL15649. In addition, substitution of Gly^{82} with Arg in SL15649 increased virus binding to heparin, suggesting an increase in E2 affinity for GAGs.

It has been hypothesized that Arg^{82} in E2 of 181/25 contributes to attenuation of the vaccine strain due to GAG binding (76, 80). Our results provide support for this hypothesis. An arginine at position 82 in both 181/25 and SL15649 results in a greater dependence on GAGs for infection in cell culture. In addition, we provide the first evidence for a direct interaction between 181/25 and an immobilized GAG, which is highly dependent on the presence of an arginine at position 82 in E2. In comparison to its parental strain AF15561, 181/25 contains 10 nucleotide differences, including two amino acid polymorphisms in the E2 glycoprotein (T12I and G82R) (80). Genetic analysis reveals that E2 T12I and G82R are responsible for attenuation of both AF15661 and a clinical isolate, CHIKV LR2006 OPY-1 (strain LR), in mouse models of CHIKV virulence (80), indicating that Arg^{82} in E2 functions in attenuation of CHIKV. Although infection of mice with 181/25 results in decreased dissemination and viremia compared with parental strain AF15561 or strain LR (76, 80), mechanisms of virulence attenuation of 181/25 *in vivo* have not been fully elucidated. Similar to other GAG-binding viruses, low levels of viremia during infection with 181/25 may be due to rapid clearance of virus from the bloodstream (55, 58, 81–83).

The conservation of a glycine at position 82 in E2 suggests that this residue contributes importantly to viral fitness. Consistent with this idea, 181/25 infects *A. albopictus* C6/36 cells less efficiently than its parental virus AF15561, which contains Gly^{82} (data not shown), suggesting that an arginine at this position in E2 brings a fitness cost for replication of CHIKV in mosquito cells. In addition, evidence of reversion from Arg to Gly at position 82 in E2 of 181/25 was observed during infections of mice (80) and in one viremic vaccinee during phase II clinical trials (67), indicating that Gly^{82} is selected for *in vivo*. It is possible that the presence of Arg^{82} may alter the tertiary structure of E2, which may affect binding to other mosquito or mammalian cell receptors.

Similar to other low-passage-number isolates of EEEV and VEEV (50, 62), CHIKV SL15649 exhibits dependence on cell-surface GAGs for efficient binding and infection in cell culture. However, GAG binding may not be a property of all CHIKV strains. For example, it has been demonstrated that CHIKV strain LR replicon particles do not depend on cell-surface GAGs for infection (76). It is unclear whether the observed difference between SL15649 and LR in GAG dependence is due to sequence polymorphisms or experimental differences. Sequence analysis of the infectious clone of SL15649 did not reveal the presence of additional basic amino acids in E2 compared with other clinical isolates (data not shown), suggesting that the requirement for cell-surface GAGs for efficient infection of SL15469 is not the result of cell culture adaptation.

Our experiments using CHO cells deficient in various GAGs provide evidence that 181/25 and SL15649 are dependent on GAGs to differing extents for efficient infection. While it is possible that abrogation of GAG expression in mutant CHO cells alters the expression of other cell-surface molecules required for CHIKV binding, we think this is unlikely since CHIKV strain LR readily infects these cells (76). Interestingly, we did not detect inhibition of SL15649 infectivity by soluble GAGs. SL15649 may bind to GAGs only within the context of a proteoglycan or when expressed at the cell surface. However, we observed a low level of binding of SL15649 to immobilized heparin, which is likely due to interactions between virions and heparin and not a consequence of nonspecific binding to beads, since virus did not bind beads alone. Physiologically relevant GAG-protein interactions display affinities that can range from rather weak (dissociation constant $[K_d] > 10^{-6}$ M) to moderately strong ($K_d = \sim 10^{-9}$ M) (46). Although mounting evidence suggests that high-affinity interactions with GAGs diminish alphavirus virulence (50, 55, 57–59, 63), low-affinity interactions with GAGs may be important for replication within hosts (e.g., to mediate attachment in specific tissues) and consequent pathology.

The structural specificity of the interactions between viruses and GAGs is poorly understood (reviewed in references 84 and 85). GAGs are heterogenous and differ in chain lengths, sulfation patterns, and subunit configurations due to the spatiotemporal expression patterns of GAG biosynthesis genes (79, 85, 86). The presence of specific subunits (e.g., iduronic acid) (44, 87) or the extent and position of sulfation of particular GAGs (39, 88, 89) can substantially influence the specificity of virus-GAG interactions. GAG-binding sites on proteins are surface exposed or in shallow grooves containing positively charged amino acids. The precise spacing of cationic clusters and the composition and arrangement of other residues that comprise the local environment of the GAG-binding site are important for specificity of interactions with GAGs (49, 90). Strain variants that contain basic residues that mediate some level of GAG binding among the different alphaviruses map to five surface-exposed regions within E2: residues 1 to 4 (53–55, 62), 70 to 82 (50, 53–55, 58–60), 114 to 120 (53, 55, 62), 157 to 161 (58), and 209 to 218 (51, 55). Although it is thought that alphavirus E1 and E2 trimers adopt similar overall folds (30, 91), it is possible that the spacing and location of the GAG-binding residues and the local amino acid environment of these five regions in E2 contribute to the type and specificity of GAG-E2 interactions. Conserved basic residues are often found

within or near these five sites, which may mediate low-affinity interactions with GAGs. Basic amino acid polymorphisms within these regions of E2 from passaged viruses or natural isolates may increase the affinity of E2 for different GAGs or alter GAG-binding specificity.

Studies of interactions between GAGs and other alphaviruses have mainly focused on heparin or heparan sulfate. However, studies using other soluble GAGs suggest that some strains use GAGs other than heparan sulfate to bind cells. For example, SINV strain Toto1101 binds to and is inhibited by soluble dermatan sulfate in addition to heparin (52). Similarly, a subset of VEEV GAG-binding mutants inhibited by soluble heparin are also inhibited by soluble dermatan sulfate (55). Differences in structural specificities of GAG interactions with alphavirus E2 glycoproteins may influence the tropism and pathology of these GAG-binding viruses. Indeed, this idea is supported by a study of EEEV heparan sulfate-binding mutants (59).

Our data suggest that 181/25 and SL15649 differ in the utilization of individual GAGs or structural specificities of GAGs. Although 181/25 infectivity was inhibited to some extent by all soluble GAGs tested, regardless of type of subunits or level of sulfation, this virus displays greater GAG specificity in cell culture. Based on studies using mutant CHO cell lines, strain 181/25 appears to depend mainly on heparan sulfate in cell culture, whereas SL15649 appears to use chondroitin sulfate, possibly in addition to heparan sulfate, for infection. Whether the amino acid sequences that influence GAG dependence for 181/25 and SL15649 are distinct or contiguous remains to be determined. Interestingly, E2 from 181/25 and SL15469 contains a heparin-binding consensus sequence (47) (from residues 250 to 255 [DRKGKI]) which is solvent accessible and conserved in other circulating CHIKV isolates. Ongoing work to define GAG-binding sites and structural specificity of GAG interactions with CHIKV 181/25 and virulent clinical isolates will enhance an understanding of CHIKV tropism and pathogenesis.

ACKNOWLEDGMENTS

We thank Andrea Pruijssers and Bernardo Mainou for critical reviews of the manuscript. We are grateful to members of the Dermody laboratory for useful suggestions and discussions during the course of the study. We thank Nicole Sexton for technical assistance. We thank Kerstin Reiss and Melanie Dietrich from the laboratory of Thilo Stehle for their assistance with structural analysis. A subset of infectivity assays were conducted at the Vanderbilt High-Throughput Screening Facility. Flow cytometry experiments were performed in the Vanderbilt Cytometry Shared Resource.

This work was supported by Public Health Service awards F32 AI096833 (L.A.S.) and U54 AI057157 for the Southeast Regional Center for Excellence for Emerging Infections and Biodefense (T.S.D.) and the Elizabeth B. Lamb Center for Pediatric Research. Additional support by provided by the Vanderbilt Diabetes Research and Training Center for the Vanderbilt Flow Cytometry Shared Resource (DK058404).

REFERENCES

1. **Burt FJ, Rolph MS, Rulli NE, Mahalingam S, Heise MT.** 2012. Chikungunya: a re-emerging virus. Lancet **379:**662–671. http://dx.doi.org/10.1016/S0140-6736(11)60281-X.
2. **Thiberville SD, Moyen N, Dupuis-Maguiraga L, Nougairede A, Gould EA, Roques P, de Lamballerie X.** 2013. Chikungunya fever: epidemiology, clinical syndrome, pathogenesis and therapy. Antiviral Res. **99:**345–370. http://dx.doi.org/10.1016/j.antiviral.2013.06.009.
3. **Schwartz O, Albert ML.** 2010. Biology and pathogenesis of chikungunya virus. Nat. Rev. Microbiol. **8:**491–500. http://dx.doi.org/10.1038/nrmicro2368.
4. **Borgherini G, Poubeau P, Jossaume A, Gouix A, Cotte L, Michault A, Arvin-Berod C, Paganin F.** 2008. Persistent arthralgia associated with chikungunya virus: a study of 88 adult patients on reunion island. Clin. Infect. Dis. **47:**469–475. http://dx.doi.org/10.1086/590003.
5. **Couturier E, Guillemin F, Mura M, Leon L, Virion JM, Letort MJ, De Valk H, Simon F, Vaillant V.** 2012. Impaired quality of life after chikungunya virus infection: a 2-year follow-up study. Rheumatology (Oxford) **51:**1315–1322. http://dx.doi.org/10.1093/rheumatology/kes015.
6. **Hoarau JJ, Jaffar Bandjee MC, Krejbich Trotot P, Das T, Li-Pat-Yuen G, Dassa B, Denizot M, Guichard E, Ribera A, Henni T, Tallet F, Moiton MP, Gauzere BA, Bruniquet S, Jaffar Bandjee Z, Morbidelli P, Martigny G, Jolivet M, Gay F, Grandadam M, Tolou H, Vieillard V, Debre P, Autran B, Gasque P.** 2010. Persistent chronic inflammation and infection by Chikungunya arthritogenic alphavirus in spite of a robust host immune response. J. Immunol. **184:**5914–5927. http://dx.doi.org/10.4049/jimmunol.0900255.
7. **Schilte C, Staikowsky F, Couderc T, Madec Y, Carpentier F, Kassab S, Albert ML, Lecuit M, Michault A.** 2013. Chikungunya virus-associated long-term arthralgia: a 36-month prospective longitudinal study. PLoS Negl. Trop. Dis. **7:**e2137. http://dx.doi.org/10.1371/journal.pntd.0002137.
8. **Sissoko D, Malvy D, Ezzedine K, Renault P, Moscetti F, Ledrans M, Pierre V.** 2009. Post-epidemic Chikungunya disease on Reunion Island: course of rheumatic manifestations and associated factors over a 15-month period. PLoS Negl. Trop. Dis. **3:**e389. http://dx.doi.org/10.1371/journal.pntd.0000389.
9. **Banerjee K, Mourja DT, Malunjkar AS.** 1988. Susceptibility & transmissibility of different geographical strains of Aedes aegypti mosquitoes to Chikungunya virus. Indian J. Med. Res. **87:**134–138.
10. **Singh KR, Pavri KM.** 1967. Experimental studies with chikungunya virus in Aedes aegypti and Aedes albopictus. Acta Virol. **11:**517–526.
11. **Tesh RB, Gubler DJ, Rosen L.** 1976. Variation among goegraphic strains of Aedes albopictus in susceptibility to infection with chikungunya virus. Am. J. Trop. Med. Hyg. **25:**326–335.
12. **Tsetsarkin KA, Vanlandingham DL, McGee CE, Higgs S.** 2007. A single mutation in chikungunya virus affects vector specificity and epidemic potential. PLoS Pathog. **3:**e201. http://dx.doi.org/10.1371/journal.ppat.0030201.
13. **Sourisseau M, Schilte C, Casartelli N, Trouillet C, Guivel-Benhassine F, Rudnicka D, Sol-Foulon N, Le Roux K, Prevost MC, Fsihi H, Frenkiel MP, Blanchet F, Afonso PV, Ceccaldi PE, Ozden S, Gessain A, Schuffenecker I, Verhasselt B, Zamborlini A, Saib A, Rey FA, Arenzana-Seisdedos F, Despres P, Michault A, Albert ML, Schwartz O.** 2007. Characterization of reemerging chikungunya virus. PLoS Pathog. **3:**e89. http://dx.doi.org/10.1371/journal.ppat.0030089.
14. **Borgherini G, Poubeau P, Staikowsky F, Lory M, Le Moullec N, Becquart JP, Wengling C, Michault A, Paganin F.** 2007. Outbreak of chikungunya on Reunion Island: early clinical and laboratory features in 157 adult patients. Clin. Infect. Dis. **44:**1401–1407. http://dx.doi.org/10.1086/517537.
15. **Economopoulou A, Dominguez M, Helynck B, Sissoko D, Wichmann O, Quenel P, Germonneau P, Quatresous I.** 2009. Atypical Chikungunya virus infections: clinical manifestations, mortality and risk factors for severe disease during the 2005–2006 outbreak on Reunion. Epidemiol. Infect. **137:**534–541. http://dx.doi.org/10.1017/S0950268808001167.
16. **Rajapakse S, Rodrigo C, Rajapakse A.** 2010. Atypical manifestations of chikungunya infection. Trans. R. Soc. Trop. Med. Hyg. **104:**89–96. http://dx.doi.org/10.1016/j.trstmh.2009.07.031.
17. **Das T, Jaffar-Bandjee MC, Hoarau JJ, Krejbich Trotot P, Denizot M, Lee-Pat-Yuen G, Sahoo R, Guiraud P, Ramful D, Robin S, Alessandri JL, Gauzere BA, Gasque P.** 2010. Chikungunya fever: CNS infection and pathologies of a re-emerging arbovirus. Prog. Neurobiol. **91:**121–129. http://dx.doi.org/10.1016/j.pneurobio.2009.12.006.
18. **Dupont-Rouzeyrol M, Caro V, Guillaumot L, Vazeille M, D'Ortenzio E, Thiberge JM, Baroux N, Gourinat AC, Grandadam M, Failloux AB.** 2012. Chikungunya virus and the mosquito vector Aedes aegypti in New Caledonia (South Pacific Region). Vector Borne Zoonotic Dis. **12:**1036–1041. http://dx.doi.org/10.1089/vbz.2011.0937.
19. **Horwood PF, Reimer LJ, Dagina R, Susapu M, Bande G, Katusele M, Koimbu G, Jimmy S, Ropa B, Siba PM, Pavlin BI.** 2013. Outbreak of chikungunya virus infection, Vanimo, Papua New Guinea. Emerg. Infect. Dis. **19:**1535–1538. http://dx.doi.org/10.3201/eid1909.130130.
20. **Mombouli JV, Bitsindou P, Elion DO, Grolla A, Feldmann H, Niama FR, Parra HJ, Munster VJ.** 2013. Chikungunya virus infection, Brazza-

ville, Republic of Congo, 2011. Emerg. Infect. Dis. **19:**1542–1543. http://dx.doi.org/10.3201/eid1909.130451.
21. **Wangchuk S, Chinnawirotpisan P, Dorji T, Tobgay T, Dorji T, Yoon IK, Fernandez S.** 2013. Chikungunya fever outbreak, Bhutan, 2012. Emerg. Infect. Dis. **19:**1681–1684. http://dx.doi.org/10.3201/eid1910.130453.
22. **Wu D, Zhang Y, Zhouhui Q, Kou J, Liang W, Zhang H, Monagin C, Zhang Q, Li W, Zhong H, He J, Li H, Cai S, Ke C, Lin J.** 2013. Chikungunya virus with E1-A226V mutation causing two outbreaks in 2010, Guangdong, China. Virol. J. **10:**174. http://dx.doi.org/10.1186/1743-422X-10-174.
23. **Thiberville SD, Boisson V, Gaudart J, Simon F, Flahault A, de Lamballerie X.** 2013. Chikungunya fever: a clinical and virological investigation of outpatients on Reunion Island, South-West Indian Ocean. PLoS Negl. Trop. Dis. **7:**e2004. http://dx.doi.org/10.1371/journal.pntd.0002004.
24. **Kuhn RJ.** 2007. Togaviridae: the viruses and their replication, p 1001–1022. *In* Knipe DM, Howley PM, Griffin DE, Lamb RA, Martin MA, Roizman B, Straus SE (ed), Fields virology, 5th ed. Lippincott, Williams and Wilkins, New York, NY.
25. **Khan AH, Morita K, Parquet Md Mdel C, Hasebe F, Mathenge EG, Igarashi A.** 2002. Complete nucleotide sequence of chikungunya virus and evidence for an internal polyadenylation site. J. Gen. Virol. **83**(Pt 12)**:**3075–3084.
26. **Fuller SD.** 1987. The T=4 envelope of Sindbis virus is organized by interactions with a complementary T=3 capsid. Cell **48:**923–934. http://dx.doi.org/10.1016/0092-8674(87)90701-X.
27. **Mancini EJ, Clarke M, Gowen BE, Rutten T, Fuller SD.** 2000. Cryo-electron microscopy reveals the functional organization of an enveloped virus, Semliki Forest virus. Mol. Cell **5:**255–266. http://dx.doi.org/10.1016/S1097-2765(00)80421-9.
28. **Sun S, Xiang Y, Akahata W, Holdaway H, Pal P, Zhang X, Diamond MS, Nabel GJ, Rossmann MG.** 2013. Structural analyses at pseudo atomic resolution of Chikungunya virus and antibodies show mechanisms of neutralization. eLife **2:**e00435. http://dx.doi.org/10.7554/eLife.00435.
29. **Jose J, Snyder JE, Kuhn RJ.** 2009. A structural and functional perspective of alphavirus replication and assembly. Future Microbiol. **4:**837–856. http://dx.doi.org/10.2217/fmb.09.59.
30. **Voss JE, Vaney MC, Duquerroy S, Vonrhein C, Girard-Blanc C, Crublet E, Thompson A, Bricogne G, Rey FA.** 2010. Glycoprotein organization of Chikungunya virus particles revealed by X-ray crystallography. Nature **468:**709–712. http://dx.doi.org/10.1038/nature09555.
31. **Kielian M, Chanel-Vos C, Liao M.** 2010. Alphavirus entry and membrane fusion. Viruses **2:**796–825. http://dx.doi.org/10.3390/v2040796.
32. **Bernard E, Solignat M, Gay B, Chazal N, Higgs S, Devaux C, Briant L.** 2010. Endocytosis of chikungunya virus into mammalian cells: role of clathrin and early endosomal compartments. PLoS One **5:**e11479. http://dx.doi.org/10.1371/journal.pone.0011479.
33. **Gay B, Bernard E, Solignat M, Chazal N, Devaux C, Briant L.** 2012. pH-dependent entry of chikungunya virus into Aedes albopictus cells. Infect. Genet. Evol. **12:**1275–1281. http://dx.doi.org/10.1016/j.meegid.2012.02.003.
34. **Lee RC, Hapuarachchi HC, Chen KC, Hussain KM, Chen H, Low SL, Ng LC, Lin R, Ng MM, Chu JJ.** 2013. Mosquito cellular factors and functions in mediating the infectious entry of chikungunya virus. PLoS Negl. Trop. Dis. **7:**e2050. http://dx.doi.org/10.1371/journal.pntd.0002050.
35. **Haywood AM.** 1994. Virus receptors: binding, adhesion strengthening, and changes in viral structure. J. Virol. **68:**1–5.
36. **Mercer J, Schelhaas M, Helenius A.** 2010. Virus entry by endocytosis. Annu. Rev. Biochem. **79:**803–833. http://dx.doi.org/10.1146/annurev-biochem-060208-104626.
37. **Dechecchi MC, Tamanini A, Bonizzato A, Cabrini G.** 2000. Heparan sulfate glycosaminoglycans are involved in adenovirus type 5 and 2-host cell interactions. Virology **268:**382–390. http://dx.doi.org/10.1006/viro.1999.0171.
38. **Zautner AE, Korner U, Henke A, Badorff C, Schmidtke M.** 2003. Heparan sulfates and coxsackievirus-adenovirus receptor: each one mediates coxsackievirus B3 PD infection. J. Virol. **77:**10071–10077. http://dx.doi.org/10.1128/JVI.77.18.10071-10077.2003.
39. **Chen Y, Maguire T, Hileman RE, Fromm JR, Esko JD, Linhardt RJ, Marks RM.** 1997. Dengue virus infectivity depends on envelope protein binding to target cell heparan sulfate. Nat. Med. **3:**866–871. http://dx.doi.org/10.1038/nm0897-866.
40. **Tan CW, Poh CL, Sam IC, Chan YF.** 2013. Enterovirus 71 uses cell surface heparan sulfate glycosaminoglycan as an attachment receptor. J. Virol. **87:**611–620. http://dx.doi.org/10.1128/JVI.02226-12.
41. **WuDunn D, Spear PG.** 1989. Initial interaction of herpes simplex virus with cells is binding to heparan sulfate. J. Virol. **63:**52–58.
42. **Roderiquez G, Oravecz T, Yanagishita M, Bou-Habib DC, Mostowski H, Norcross MA.** 1995. Mediation of human immunodeficiency virus type 1 binding by interaction of cell surface heparan sulfate proteoglycans with the V3 region of envelope gp120-gp41. J. Virol. **69:**2233–2239.
43. **Giroglou T, Florin L, Schafer F, Streeck RE, Sapp M.** 2001. Human papillomavirus infection requires cell surface heparan sulfate. J. Virol. **75:**1565–1570. http://dx.doi.org/10.1128/JVI.75.3.1565-1570.2001.
44. **Hallak LK, Collins PL, Knudson W, Peeples ME.** 2000. Iduronic acid-containing glycosaminoglycans on target cells are required for efficient respiratory syncytial virus infection. Virology **271:**264–275. http://dx.doi.org/10.1006/viro.2000.0293.
45. **Esko JD, Kimata K, Lindahl U.** 2009. Proteoglycans and sulfated glycosaminoglycans, p 229–248. *In* Varki A, Cummings RD, Esko JD, Freeze HH, Stanley P, Bertozzi CR, Hart GW, Etzler ME (ed), Essentials of glycobiology, 2nd ed. Cold Spring Harbor Laboratory Press, Cold Spring Harbor, NY.
46. **Gandhi NS, Mancera RL.** 2008. The structure of glycosaminoglycans and their interactions with proteins. Chem. Biol. Drug Des. **72:**455–482. http://dx.doi.org/10.1111/j.1747-0285.2008.00741.x.
47. **Cardin AD, Weintraub HJ.** 1989. Molecular modeling of protein-glycosaminoglycan interactions. Arteriosclerosis **9:**21–32. http://dx.doi.org/10.1161/01.ATV.9.1.21.
48. **Hileman RE, Fromm JR, Weiler JM, Linhardt RJ.** 1998. Glycosaminoglycan-protein interactions: definition of consensus sites in glycosaminoglycan binding proteins. Bioessays **20:**156–167. http://dx.doi.org/10.1002/(SICI)1521-1878(199802)20:2<156::AID-BIES8>3.0.CO;2-R.
49. **Torrent M, Nogues MV, Andreu D, Boix E.** 2012. The "CPC clip motif": a conserved structural signature for heparin-binding proteins. PLoS One **7:**e42692. http://dx.doi.org/10.1371/journal.pone.0042692.
50. **Gardner CL, Ebel GD, Ryman KD, Klimstra WB.** 2011. Heparan sulfate binding by natural eastern equine encephalitis viruses promotes neurovirulence. Proc. Natl. Acad. Sci. U. S. A. **108:**16026–16031. http://dx.doi.org/10.1073/pnas.1110617108.
51. **Heil ML, Albee A, Strauss JH, Kuhn RJ.** 2001. An amino acid substitution in the coding region of the E2 glycoprotein adapts Ross River virus to utilize heparan sulfate as an attachment moiety. J. Virol. **75:**6303–6309. http://dx.doi.org/10.1128/JVI.75.14.6303-6309.2001.
52. **Byrnes AP, Griffin DE.** 1998. Binding of Sindbis virus to cell surface heparan sulfate. J. Virol. **72:**7349–7356.
53. **Klimstra WB, Ryman KD, Johnston RE.** 1998. Adaptation of Sindbis virus to BHK cells selects for use of heparan sulfate as an attachment receptor. J. Virol. **72:**7357–7366.
54. **Smit JM, Waarts BL, Kimata K, Klimstra WB, Bittman R, Wilschut J.** 2002. Adaptation of alphaviruses to heparan sulfate: interaction of Sindbis and Semliki forest viruses with liposomes containing lipid-conjugated heparin. J. Virol. **76:**10128–10137. http://dx.doi.org/10.1128/JVI.76.20.10128-10137.2002.
55. **Bernard KA, Klimstra WB, Johnston RE.** 2000. Mutations in the E2 glycoprotein of Venezuelan equine encephalitis virus confer heparan sulfate interaction, low morbidity, and rapid clearance from blood of mice. Virology **276:**93–103. http://dx.doi.org/10.1006/viro.2000.0546.
56. **Kerr PJ, Weir RC, Dalgarno L.** 1993. Ross River virus variants selected during passage in chick embryo fibroblasts: serological, genetic, and biological changes. Virology **193:**446–449. http://dx.doi.org/10.1006/viro.1993.1143.
57. **Bear JS, Byrnes AP, Griffin DE.** 2006. Heparin-binding and patterns of virulence for two recombinant strains of Sindbis virus. Virology **347:**183–190. http://dx.doi.org/10.1016/j.virol.2005.11.034.
58. **Byrnes AP, Griffin DE.** 2000. Large-plaque mutants of Sindbis virus show reduced binding to heparan sulfate, heightened viremia, and slower clearance from the circulation. J. Virol. **74:**644–651. http://dx.doi.org/10.1128/JVI.74.2.644-651.2000.
59. **Gardner CL, Choi-Nurvitadhi J, Sun C, Bayer A, Hritz J, Ryman KD, Klimstra WB.** 2013. Natural variation in the heparan sulfate binding domain of the eastern equine encephalitis virus E2 glycoprotein alters interactions with cell surfaces and virulence in mice. J. Virol. **87:**8582–8590. http://dx.doi.org/10.1128/JVI.00937-13.
60. **Klimstra WB, Heidner HW, Johnston RE.** 1999. The furin protease cleavage recognition sequence of Sindbis virus PE2 can mediate virion attachment to cell surface heparan sulfate. J. Virol. **73:**6299–6306.

61. **Ryman KD, Gardner CL, Burke CW, Meier KC, Thompson JM, Klimstra WB.** 2007. Heparan sulfate binding can contribute to the neurovirulence of neuroadapted and nonneuroadapted Sindbis viruses. J. Virol. **81:**3563–3573. http://dx.doi.org/10.1128/JVI.02494-06.
62. **Wang E, Brault AC, Powers AM, Kang W, Weaver SC.** 2003. Glycosaminoglycan binding properties of natural venezuelan equine encephalitis virus isolates. J. Virol. **77:**1204–1210. http://dx.doi.org/10.1128/JVI.77.2.1204-1210.2003.
63. **Klimstra WB, Ryman KD, Bernard KA, Nguyen KB, Biron CA, Johnston RE.** 1999. Infection of neonatal mice with sindbis virus results in a systemic inflammatory response syndrome. J. Virol. **73:**10387–10398.
64. **Morrison TE, Oko L, Montgomery SA, Whitmore AC, Lotstein AR, Gunn BM, Elmore SA, Heise MT.** 2011. A mouse model of chikungunya virus-induced musculoskeletal inflammatory disease: evidence of arthritis, tenosynovitis, myositis, and persistence. Am. J. Pathol. **178:**32–40. http://dx.doi.org/10.1016/j.ajpath.2010.11.018.
65. **Levitt NH, Ramsburg HH, Hasty SE, Repik PM, Cole FE, Jr, Lupton HW.** 1986. Development of an attenuated strain of chikungunya virus for use in vaccine production. Vaccine **4:**157–162. http://dx.doi.org/10.1016/0264-410X(86)90003-4.
66. **Edelman R, Tacket CO, Wasserman SS, Bodison SA, Perry JG, Mangiafico JA.** 2000. Phase II safety and immunogenicity study of live chikungunya virus vaccine TSI-GSD-218. Am. J. Trop. Med. Hyg. **62:**681–685.
67. **Hoke CH, Jr, Pace-Templeton J, Pittman P, Malinoski FJ, Gibbs P, Ulderich T, Mathers M, Fogtman B, Glass P, Vaughn DW.** 2012. US Military contributions to the global response to pandemic chikungunya. Vaccine **30:**6713–6720. http://dx.doi.org/10.1016/j.vaccine.2012.08.025.
68. **Mainou B, Zamora PF, Ashbrook AW, Dorset DC, Kim KS, Dermody TS.** 2013. Reovirus cell entry requires functional microtubules. mBio **4:**e00405–13. http://dx.doi.org/10.1128/mBio.00405-13.
69. **Schneider CA, Rasband WS, Eliceiri KW.** 2012. NIH Image to ImageJ: 25 years of image analysis. Nat. Methods **9:**671–675. http://dx.doi.org/10.1038/nmeth.2089.
70. **Emsley P, Cowtan K.** 2004. Coot: model building tools for molecular graphics. Acta Crystallogr. D Biol. Crystallogr. **60:**2126–2132. http://dx.doi.org/10.1107/S0907444904019158.
71. **Baker NA, Sept D, Joseph S, Holst MJ, McCammon JA.** 2001. Electrostatics of nanosystems: application to microtubules and the ribosome. Proc. Natl. Acad. Sci. U. S. A. **98:**10037–10041. http://dx.doi.org/10.1073/pnas.181342398.
72. **Pickett BE, Sadat EL, Zhang Y, Noronha JM, Squires RB, Hunt V, Liu M, Kumar S, Zaremba S, Gu Z, Zhou L, Larson CN, Dietrich J, Klem EB, Scheuermann RH.** 2012. ViPR: an open bioinformatics database and analysis resource for virology research. Nucleic Acids Res. **40:**D593–D598. http://dx.doi.org/10.1093/nar/gkr859.
73. **Ohkuma S, Poole B.** 1978. Fluorescence probe measurement of the intralysosomal pH in living cells and the perturbation of pH by various agents. Proc. Natl. Acad. Sci. U. S. A. **75:**3327–3331. http://dx.doi.org/10.1073/pnas.75.7.3327.
74. **Esko JD, Stewart TE, Taylor WH.** 1985. Animal cell mutants defective in glycosaminoglycan biosynthesis. Proc. Natl. Acad. Sci. U. S. A. **82:**3197–3201. http://dx.doi.org/10.1073/pnas.82.10.3197.
75. **Esko JD, Weinke JL, Taylor WH, Ekborg G, Roden L, Anantharamaiah G, Gawish A.** 1987. Inhibition of chondroitin and heparan sulfate biosynthesis in Chinese hamster ovary cell mutants defective in galactosyltransferase I. J. Biol. Chem. **262:**12189–12195.
76. **Gardner CL, Burke CW, Higgs ST, Klimstra WB, Ryman KD.** 2012. Interferon-alpha/beta deficiency greatly exacerbates arthritogenic disease in mice infected with wild-type chikungunya virus but not with the cell culture-adapted live-attenuated 181/25 vaccine candidate. Virology **425:**103–112. http://dx.doi.org/10.1016/j.virol.2011.12.020.
77. **Lidholt K, Weinke JL, Kiser CS, Lugemwa FN, Bame KJ, Cheifetz S, Massague J, Lindahl U, Esko JD.** 1992. A single mutation affects both N-acetylglucosaminyltransferase and glucuronosyltransferase activities in a Chinese hamster ovary cell mutant defective in heparan sulfate biosynthesis. Proc. Natl. Acad. Sci. U. S. A. **89:**2267–2271. http://dx.doi.org/10.1073/pnas.89.6.2267.
78. **Lee CY, Kam YW, Fric J, Malleret B, Koh EG, Prakash C, Huang W, Lee WW, Lin C, Lin RT, Renia L, Wang CI, Ng LF, Warter L.** 2011. Chikungunya virus neutralization antigens and direct cell-to-cell transmission are revealed by human antibody-escape mutants. PLoS Pathog. **7:**e1002390. http://dx.doi.org/10.1371/journal.ppat.1002390.
79. **Raman R, Sasisekharan V, Sasisekharan R.** 2005. Structural insights into biological roles of protein-glycosaminoglycan interactions. Chem. Biol. **12:**267–277. http://dx.doi.org/10.1016/j.chembiol.2004.11.020.
80. **Gorchakov R, Wang E, Leal G, Forrester NL, Plante K, Rossi SL, Partidos CD, Adams AP, Seymour RL, Weger J, Borland EM, Sherman MB, Powers AM, Osorio JE, Weaver SC.** 2012. Attenuation of Chikungunya virus vaccine strain 181/clone 25 is determined by two amino acid substitutions in the E2 envelope glycoprotein. J. Virol. **86:**6084–6096. http://dx.doi.org/10.1128/JVI.06449-11.
81. **Lee E, Hall RA, Lobigs M.** 2004. Common E protein determinants for attenuation of glycosaminoglycan-binding variants of Japanese encephalitis and West Nile viruses. J. Virol. **78:**8271–8280. http://dx.doi.org/10.1128/JVI.78.15.8271-8280.2004.
82. **Lee E, Lobigs M.** 2002. Mechanism of virulence attenuation of glycosaminoglycan-binding variants of Japanese encephalitis virus and Murray Valley encephalitis virus. J. Virol. **76:**4901–4911. http://dx.doi.org/10.1128/JVI.76.10.4901-4911.2002.
83. **Lee E, Wright PJ, Davidson A, Lobigs M.** 2006. Virulence attenuation of Dengue virus due to augmented glycosaminoglycan-binding affinity and restriction in extraneural dissemination. J. Gen. Virol. **87:**2791–2801. http://dx.doi.org/10.1099/vir.0.82164-0.
84. **Liu J, Thorp SC.** 2002. Cell surface heparan sulfate and its roles in assisting viral infections. Med. Res. Rev. **22:**1–25. http://dx.doi.org/10.1002/med.1026.
85. **Kamhi E, Joo EJ, Dordick JS, Linhardt RJ.** 2013. Glycosaminoglycans in infectious disease. Biol. Rev. Camb. Philos. Soc. **88:**928–943. http://dx.doi.org/10.1111/brv.12034.
86. **Esko JD, Linhardt RJ.** 2009. Proteins that bind sulfated glycosaminoglycans, p 501–511. *In* Varki A, Esko JD, Freeze HH, Stanley P, Bertozzi CR, Hart GW, Etzler ME (ed), Essentials of glycobiology, 2nd ed. Cold Spring Harbor Press, Cold Spring Harbor, NY.
87. **Thammawat S, Sadlon TA, Hallsworth PG, Gordon DL.** 2008. Role of cellular glycosaminoglycans and charged regions of viral G protein in human metapneumovirus infection. J. Virol. **82:**11767–11774. http://dx.doi.org/10.1128/JVI.01208-08.
88. **Feyzi E, Trybala E, Bergstrom T, Lindahl U, Spillmann D.** 1997. Structural requirement of heparan sulfate for interaction with herpes simplex virus type 1 virions and isolated glycoprotein C. J. Biol. Chem. **272:**24850–24857. http://dx.doi.org/10.1074/jbc.272.40.24850.
89. **Shukla D, Liu J, Blaiklock P, Shworak NW, Bai X, Esko JD, Cohen GH, Eisenberg RJ, Rosenberg RD, Spear PG.** 1999. A novel role for 3-O-sulfated heparan sulfate in herpes simplex virus 1 entry. Cell **99:**13–22. http://dx.doi.org/10.1016/S0092-8674(00)80058-6.
90. **Fromm JR, Hileman RE, Caldwell EE, Weiler JM, Linhardt RJ.** 1997. Pattern and spacing of basic amino acids in heparin binding sites. Arch. Biochem. Biophys. **343:**92–100. http://dx.doi.org/10.1006/abbi.1997.0147.
91. **Li L, Jose J, Xiang Y, Kuhn RJ, Rossmann MG.** 2010. Structural changes of envelope proteins during alphavirus fusion. Nature **468:**705–708. http://dx.doi.org/10.1038/nature09546.